Am J Cancer Res 2022;12(1):229-246
www.ajcr.us /ISSN:2156-6976/ajcr0126264

Original Article

5-arylalkynyl-2-benzoyl thiophene: a novel microtubule inhibitor exhibits antitumor activity without neurological toxicity

Yuxin Zhuang[1,2*], Guang Yang[1,3*], Shaoyu Wu[1], Jianjun Chen[1], Jiayin Guo[1], Dongling Quan[1], Tingting Zhang[1], Zichao Yang[1], Shaobin Tan[1], Yuheng Ji[1], Zhipeng Chen[1], Lin Lv[1]

[1]School of Pharmaceutical Science, Southern Medical University, Guangzhou 510515, People's Republic of China; [2]State Key Laboratory of Quality Research in Chinese Medicines, Macau Institute for Applied Research in Medicine and Health, Macau University of Science and Technology, Macau, People's Republic of China; [3]Zhuhai People's Hospital (Zhuhai Hospital Affiliated with Jinan University), Zhuhai 519000, People's Republic of China. [*]Equal contributors.

Received November 14, 2020; Accepted June 15, 2021; Epub January 15, 2022; Published January 30, 2022

Abstract: The composition of microtubules involving several steps, including the polymerization and depolymerization of α-tubulin and β-tubulin heterodimers. Microtubule-targeting agents can increase or inhibit microtubule polymerization, thereby disrupting the dynamic process and stalling cells in G2/M phase. Microtubule-targeting agents are generally cytotoxic, which neurological toxicity being one of the significant adverse events associated. We recently reported a novel 5-arylalkynyl-2-benzoyl thiophene (PST-3) that exhibited broad-spectrum cellular cytotoxicity and *in vivo* potency with high safety. PST-3 was a substrate of p-gp, which could not cross the blood-brain barrier and lead to less neurotoxicity. The antitumor activities *in vitro* demonstrated that PST-3 combined with the colchicine-binding site on microtubule, induces morphological changes, disrupts microtubule networks, inhibits polymerization of tubulin, arrests breast cancer cells in the G2/M phase of the cell cycle and induces apoptosis. Evaluation of the antitumor effect *in vivo* demonstrated that PST-3 elicited MDA-MB-468 tumor %T/C of 11.75%, whereas elicited MCF7 tumor %T/C of 44.38% in breast cancer xenograft models. Besides, *in vivo* experiments of a higher dose (60 mg/kg) of PST-3 treatment for 21 days did not produce any significant neurotoxicity. These results provide evidence that PST-3 might possess the potential to be developed into a new microtubule inhibitor without neurological toxicity.

Keywords: Microtubule inhibitor, breast cancer, neurological toxicity

Introduction

Microtubules are cytoskeletal structures composed of α-tubulin and β-tubulin heterodimers, participate in various intracellular processes and functions of cells [1-9]. Microtubules play a significant role in the becoming of the mitotic spindle, are vital for the mitosis of cells [10-17]. Therefore, disrupt tubulin polymerization can arrest cell cycle or induce apoptosis [18-20]. Accordingly, tubules became an effective target for the design as well as synthesis of a diverse novel natural or synthetic antineoplastic medicines, including combretastatin A-4, paclitaxel, epothilone B, vinblastine, and colchicine in the past decades [21-27].

Tubulin targeting inhibitors are widely used in human cancer chemotherapy. This type of anti-cancer agents destroys microtubule dynamics by binding to tubulin at four known binding sites: vinca alkaloid, taxane/epothilone, laulimalide, and colchicine sites [28]. Among all the different classes of tubulin binding compound, colchicine binding site inhibitors failed to reach clinical application stage, though a great number of potential colchicine binding site agents were synthesized and investigated to looking for a more effective and less toxic clinical medicine for cancer treatment [19]. Along with the research on numerous microtubule colchicine pocket ligand binding crystal structures gets deeper over the past decade, structurally diverse agents target to colchicine binding site were discovered or synthesized. Meanwhile, many of them show strong effectiveness and drug-like properties for preclinical applications, such as Combretastatin A-4, Arylthioindole, and

Chalcones [29, 30]. Many structurally diverse colchicine site binding agents arrest the cell cycle and inhibit cancer cells' growth. Thus, these drugs are expected to become a new serious of anticancer drugs [30]. However, many potent microtubule-binding agents have discontinued evaluating due to significant peripheral neurotoxicity [22]. The major shortcoming of using drugs that target tubule is the high incidence of neuropathy follow by the applying of such agents [31]. The potential side effect that limited by dose accumulates during the treatment of cancer patients accompanied by pre-existing neuropathy and generally manifested as peripheral neuropathy with pain, weakness, and constipation caused by toxicity to the autonomic nervous system or Intestinal paralysis for which lack of effective symptomatic treatment at present [32, 33]. Some patients still have severe neurological sequelae several years after the end of treatment. Therefore, it is imperative to search for novel microtubule inhibitors with low peripheral neurotoxicity.

During the screening of microtubule-targeting agents using the molecular docking study, we found an active sample designated PST-3 combined with the colchicine-binding site of the microtubule. This thiophene compound, verified as (2-(3, 4-Dimethoxy)-benzoyl)-(5-(4-ethyl)-phenylethynyl)-thiophene was synthesized from 2-benzoyl-5-bromo thiophene in our laboratory (China Patent: No. ZL 201410-081034.8, Supplementary Figure 1). PST-3 is structurally similar to the SMART analogs (a series of 4-substituted methoxybenzoyl-arylthiazoles) which are also tubulin inhibitors targeting colchicine site and showed lower neurotoxicity as compared to other known tubulin inhibitors, vinblastine and colchicine for instance [30]. In summary, we propose a hypothesis that the PST-3 may also have lower neurotoxicity than colchicine when we designed the compounds. Cell Counting Kit-8 assay suggested that PST-3 could induce cytotoxicity in different cancer cell lines with limited toxicity on normal cells. Herein, our research focuses on the peripheral neurotoxicity and the antitumor mechanism of PST-3.

Materials and methods

Materials

Reagents: Cell Counting Kit-8 (CCK-8; DOJINDO); RPMI-1640 medium (Gibco, CAS# 11875-093); Fetal Bovine Serum (FBS; Capricorn Scientific, FBS-12A); 5-Fluorouracil (5-FU, CAS# 51-21-8); 2-(4-Amidinophenyl)-6-indolecarbamidine dihydrochloride (DAPI; Beyotime Biotechnology, CAS# 28718-90-3); Colchicine (Sigma, CAS# 64-86-8); Docetaxel (Sigma, CAS# 114977-28-5); Paraformaldehyde (Thermo Fisher Scientific, CAS# 30525-89-4); Triton X-100 (Aladdin, CAS# 9002-93-1); dimethyl sulfoxide (DMSO; Sigma, CAS# 67-68-5); Bovine serum albumin (BSA; Millipore, CAS# 9048-46-8). Antibodies: α-tubulin mouse monoclonal antibody (Cell Signaling Technology, 3873); β-tubulin rabbit monoclonal antibody (Cell Signaling Technology, 2128); Alexa Fluor® 555 Conjugate anti-rabbit IgG (Cell Signaling Technology, 4413S); Fluorescein isothiocyanate AffiniPure goat anti-mouse IgG (FITC; EarthOx, CAS# E031220-01).

Cells and cell culture

The following cell lines were obtained from Nanjing Cobioer Bio-Technology: BT549, Hs578T, MDA-MB-231, MDA-MB-468, T47D, MCF7, HCT-116, RKO, MIA-PaCa-2, PANC-1, A549, HeLa, and MCF10A. Cells were authenticated by STR Short tandem repeats (STR) standard conducted by Nanjing Cobioer Bio-Technology and used within 6 months. Mycoplasma testing regimen was carried under the manufacturer's instruction of MycoAlert Mycoplasma Detection Kit (Lonza, CAS# LT07-318). All breast cancer, colon cancer, non-small cell lung cancer and cervical cancer cell lines were cultured in RPMI-1640 medium supplemented with 10% FBS. All pancreatic cancer cell lines were maintained in Dulbecco's Modified Eagle's medium and 10% fetal bovine serum. MCF10A were maintained in Mammary Epithelial Cell Growth Medium and 100 ng/ml cholera toxin. The cells were cultured at 37°C in a 5% CO_2 atmosphere for the following studies.

Cell proliferation assays

Cells were cultured at 2 × 10^3 cells/well into 96-well plates and then treated with 0.1% DMSO, 5-FU (1, 3, 10, 30, or 100 μM), or PST-3 (1, 3, 10, 30, or 100 μM) for 72 h. The positive control group was treated with 5-FU and vehicle control group was treated with 0.1% DMSO. After 72 h of treatment, the cells were incubated with 10 μl of CCK-8 for 1-4 h at 37°C. The absorbance at 450 nm was measured using an OD plate reader (Bio-Rad laboratories, USA) [34].

Clonogenic assay

Breast cancer cells were plated in 6-well plates at a density of 200 cells/well. On the following day, cells were treated with PST-3 at 1, 3, 10, 30, or 50 μM for 24 hours, after which time, the growth medium was replaced. After 8 days, cell colonies were fixed with trypan blue solution (75% methanol/25% acetic acid/0.25% trypan blue), washed, and air-dried after counting colonies > 50 cells.

Acute toxicity studies

Kunming mice were grouped using a computerized randomization procedure so that the mean body weight of each group was comparable as follows: 100 KM mice were divided into 10 groups, including 5 males and 5 females. The PST-3 compound was administered intraperitoneally to mice in 0.1% Captex200/Tween80 (1/4) suspension at graded doses of 2.15, 21.5, 215 and 2150 mg/kg body weight, while the mice in the vehicle group received 0.1% Captex200/Tween80 (1/4). Colchicine was a positive control to keep the experimental conditions above unchanged. The general behavior and indicators of toxicity of the mice were investigated 3 hours after administration. Mice were further observed twice daily until 14 days to observe the changes of behavior and signs of toxicity and/or death between different groups.

Molecular docking study

Molecular docking was used to evaluate the interaction between PST-3 compound and the colchicine site receptor with Autodock Vina. First, the initial structure of the colchicine receptor (PDB ID: 1SA0) was retrieved from the Protein Data Bank [35] and then arranged for our study with AutoDockTool (ADT) 1.5.6 by removing water molecules and the colchicine structure and adding polar hydrogens. The colchicine structure was saved from the initial colchicine site receptor structure to use as a control. Moreover, the grid box was placed on the structure of colchicine and extended 5 Å from each side (box size: 68 × 70 × 60 Å and box center: 118.794 × 89.74 × 6.135 Å). All amino acids in the grid box were set as flexible residues, whereas the amino acids outside the grid box were set as rigid. The binding events were detected based on the Lamarckian version of the genetic algorithm. The PST-3 ligands were built, and the energy of PSTs was minimized using YASARA software. The docking results were imported into YASARA, Python Molecular Viewer, and LigPlus to compute the hydrogen bonding and hydrophobic interactions between each ligand and the receptor. Screenshots of the docking structures were visualized using YASARA and PyMOL.

Immunofluorescence microtubule detection

BT549 and MDA-MB-468 cells (2×10^4 cells/well) were plated on round slips. The cells were treated with PST-3 (15 and 30 μM) or 0.1% DMSO for 6 h. After treatment, the cells were washed with PBS for 3 times, fixed with 4% paraformaldehyde and then permeabilized with 0.1% Triton X-100. Cells were incubated with primary antibodies (α-tubulin mouse monoclonal antibody and β-tubulin rabbit monoclonal antibody) overnight at 4°C after blocking with 5% BSA for 1 h. After washed with PBS, cells were incubated with fluorescent secondary antibodies and DAPI. Take and analyze images by confocal microscope (Carl Zeiss LSM 880).

In vitro tubulin polymerization assay

Various concentrations of PST-3 (0.15, 0.3, 0.7, 1.5, 3, 6, 12.5, 25, 50, 100 μM) were added to PEM buffer (100 mM PIPES, 1 mM $MgCl_2$, 1 mM EGTA, 1 mM GTP and 5% glycerol) containing tubulin. Microtubule polymerization was monitored at 37°C by light scattering at 340 nm. The absorbance of platform period was used for calculations. Colchicine and docetaxel (0.15, 0.3, 0.7, 1.5, 3, 6, 12.5, 25, 50, 100 μM) were positive control, whereas DMSO (0.1%) was negative control. The experiment was repeated twice. The concentration causing a 50% inhibition (IC_{50}) of polymerization was determined, and the IC_{50} values of compounds above were compared to the IC_{50} of colchicine. All measurements were performed the same day under the same conditions.

Cell-cycle analysis

The MDA-MB-468 and BT549 cells were treated with the IC_{50} concentration of PST-3 for 12, 24, 36, 48, 60, 72 hours. After treatment, the cells were fixed by 75% ethanol. The cellular

DNA was stained with 100 μg/mL propidium iodide (PI) and 100 μg/mL RNase A in PBS at 37°C in the dark. Cell-cycle distribution of the cells was detected by flow cytometry.

Apoptosis analysis

Using Annexin V-FITC Apoptosis Detection Kit (Beyotime Biotechnology) to determine cell apoptosis. After 48 hours of treatment with PST-3, the cells were harvested and resuspended in 1 × binding buffer, followed by adding Annexin-V FITC and PI, and incubate in the dark at room temperature for 15 minutes. The proportion of apoptotic cells was determined by flow cytometry.

Immunoblotting

Cell lysate from BT549 and MDA-MB-468 cell lines was prepared after treatment with PST-3 (15 μM for 24, 48, and 72 hours). In brief, cells were harvested and washed with PBS, the supernatant was discarded, and cells were resuspended in lysis buffer (25 mM Tris (pH 7.6), 150 mM NaCl, 1% NP-40, 1% sodium deoxycholate and 0.1% SDS) containing protease inhibitors. Total protein samples were collected by centrifugation at 12,000 rpm for 30 minutes and protein concentration was measured by BSA assay. For western blotting assay, 30 μg proteins were resolved over 4-15% SDS-polyacrylamide gel. The protein was then transferred to nitrocellulose (NC) membrane (Millipore). followed by incubation with corresponding primary antibodies at 4°C overnight. Membranes were incubated with HRP-labeled secondary antibody for 1 hour at room temperature. The blots were collected and analyzed by chemiluminescent solution ImmobilonTM western (Millipore).

Animal experiment procedure ethics

All animal studies were done in accordance with protocols approved by the Institutional Animal Care and Use Committee at Southern Medical University (Resolution NO. L2016194).

Pharmacokinetic study

Kunming mice (n = 5 per group) aged 6 to 8 weeks were used to examine the pharmacokinetics of the PST-3. PST-3 (60 mg/kg) were dissolved in 0.1% Captex200/Tween80 (1/4) and administered intraperitoneally. The Dose was determined based on the acute toxicity study of PST-3 in Kunming mice (n = 10 per group), which shows that doses of 60 mg/kg result in less than 10% body weight loss after 4 consecutive days of i.p. dosing (Supplementary Table 1). Collecting blood samples at 0.5, 1, 1.5, 2, 3, 4, 6, 12, 16 and 24 hours after administration. The preparation for the sample was through protein precipitation. Adding a volume of 200 μL acetonitrile to 100 μL of plasma. The supernatant was analyzed by HPLC after centrifugation. And thus, determine the pharmacokinetic parameters using non-interventricular analysis.

Tumor xenograft studies

6 to 8-week-old female athymic nude mice were used to established MDA-MB-468, and MCF7 tumors model, 1×10^7 of cells were subcutaneous injection into the upper side of the leg in mice. The length and width (mm) of the tumor were measured each day and the volume (mm^3) of the tumor was calculated use the following formula, $\pi/6 \times L \times W^2$ (mm). The tumor-bearing animals were treated intraperitoneally (i.p.) with vehicle 0.1% Captex200/Tween80 (1/4), PST-3 (60 mg/kg) for 21 days when the tumor volumes reached 150 mm^3. Use the following parameters to assess drug effect: %T/C = [Δ tumor volume of the treated group]/[Δ tumor volume of control group] × 100%. According to National Cancer Institute criteria, compound is believed to be minimally active when conferring %T/C < 40%, and are considered to be highly active when %T/C < 10% [36].

Rotarod test

A two-day training was performed to Kunming mice, to ensure they can stand on the rotating rod for at less 2 minutes at 12 pm. Mice were divided into 5 mice per group randomly assigned based on the duration they stay on the rotating rod. Mice were treated with PST-3 in 0.1% Captex200/Tween80 (1/4) at 20, 40 or 60 mg/kg by intraperitoneal injection. Under the same conditions, Colchicine at 0.05 mg/kg/day (maximum tolerated dose) was a positive control [37]. Carry the rotating experience two times a week. Moreover, stopped on the 21st day, post-observation was tested at 1, 2, and 4 weeks once the treatment was finish.

Table 1. Effects of PST-3 compound on human cancer cells proliferation

Cell	IC_{50} (μM)	
	PST-3	5-FU
BT549	15.42±0.17	32.89±1.44
Hs578T	23.36±0.29	30.88±1.13
MDA-MB-231	32.75±0.67	40.53±2.20
MDA-MB-468	16.33±1.94	35.70±2.33
T47D	61.05±0.07	30.42±1.22
MCF7	62.05±1.55	53.59±3.06
HCT-116	37.71±1.54	47.71±2.17
RKO	29.34±0.85	41.36±1.94
MIA PaCa-2	30.82±1.45	37.17±1.29
PANC-1	44.85±0.96	31.55±2.67
A549	76.84±2.47	41.89±3.07
Hela	63.05±1.42	53.00±1.55
MCF10A	278.13±33.68	64.21±2.34

IC_{50} values denote the compound concentration that inhibits 50% of cell growth. Values represent the mean ± S.D. from 3 separate experiments.

Speed of the rod was added from 5 rpm to 40 rpm every 5 minutes. Measure the experience by the duration of mice staying on the rotating rod.

P-gp ATPase activity

PST-3 or colchicine-stimulated activity of P-gp ATPase was determined by P-gp-Glo™ assay systems. The group treated with Verapamil as a positive control and Na_3VO_4 as an inhibitor. All steps in the procedure were based on the manufacturer's instructions. The luminescence of the samples was determined by UV/VIS Spectorphotomter (TECAN, Switzerland).

Data and materials availability

All data needed to evaluate the conclusions in the paper are present in the paper and/or the Supplementary Materials. Additional data related to this paper may be requested from the authors.

Results

Cytotoxicity of PST-3 to different cancer cell with high safety

The PST-3 were screened in 12 human cancer cell lines involving in breast cancer (BT549, Hs578T, MDA-MB-231, MDA-MB-468, T47D, and MCF7), colon cancer (HCT-116 and RKO), pancreatic cancer (MIA-PaCa-2 and PANC-1), non-small cell lung cancer (A549), as well as cervical cancer (HeLa) by measuring the inhibition of proliferation. The results were listed in **Table 1**. Among the cell lines tested, BT549 and MDA-MB-468 had the highest sensitivity to PST-3, followed by Hs578T, RKO and MIA PaCa-2. 5-FU is frequently administrated as a broad-spectrum first-line treatment for cancers. The inhibitory effect of PST-3 compounds on BT549 and MDA-MB-468 cells was twice that of 5-FU. IC_{50} values of PST-3 in BT549 and MDA-MB-468 cell line were 15.42 and 16.33 μM, respectively, whereas in Hs578T, RKO and MIA PaCa-2 were 23.36, 29.34 and 30.82 μM, respectively after treating with PST-3 for 72 hours. In the cancer cell lines tested, A549 exhibited the minimum sensitivity to PST-3 (76.84 μM). Interestingly, the IC_{50} values for PST-3 were lower in Hs578T, BT549, MDA-MB-231 and MDA-MB-468 cells (Triple-negative breast cancer cell, TNBC cell) than MCF7 and T47D cells (non-TNBC cell) which indicated that PST-3 were more sensitive to TNBC cells. Moreover, the IC_{50} for PST-3 in MCF10A was 278.13±33.68 μM. As compared with various kinds of cancer cells, PST-3 has a limited killing effect on normal mammary epithelial cells MCF10A.

Colony formation experience was performed to study the influences of PST-3 on the proliferative capacity of the individual breast cancer cell. The results in **Figure 1** indicated that PST-3 suppressed clonal growth in 6 breast cancer cell lines. TNBC cells lines BT549 and MDA-MB-468, which had the highest sensitivity to PST-3, had higher IC_{50} for clonal growth than the non-TNBC cell lines MCF7 and T47D (**Table 2**). The results suggest that PST-3 can be developed as specific chemotherapy agents for those triple-negative breast cancer cells.

The toxicity of PST-3 was further examined with acute toxicity study. In the groups receiving colchicine, the death and acute toxicity raised gradually while the dosage increased from 2.15 to 2150 mg/kg (Supplementary Table 2). The observed toxic behaviors were mainly characterized by decreased exercise activity, fatigue, and lethargy. The dying mice showed asthma, abdominal breathing, convulsions, and diarrhea. Respiratory failure may be the

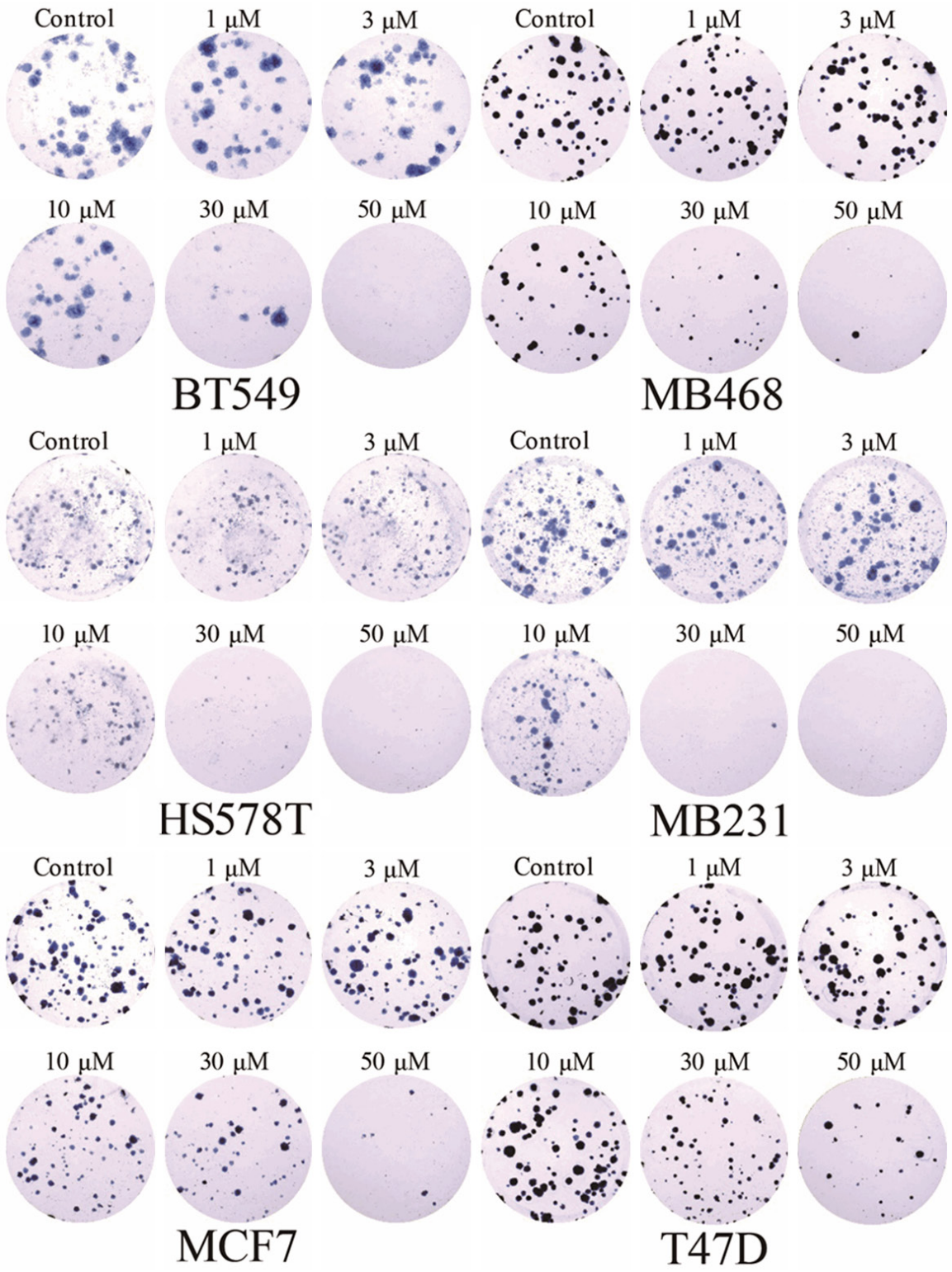

Figure 1. Images of the effect of PST-3 on breast cancer cells clonogenic growth.

cause of death. Interestingly, in the groups receiving PST-3, there was no significant acute toxicity, and all mice survived until the end of observation. The full recovery of surviving mice was 14 days later. The LD_{50} of the PST-3 and colchicine in mice were more than 2150

Table 2. Effect of PST-3 on human breast cancer cell clonogenic growth

Cell	IC_{50} (μM)
BT549	3.72±1.22
MDA-MB-468	3.42±0.83
Hs578T	11.15±0.79
MDA-MB-231	11.43±1.19
MCF7	18.79±2.58
T47D	24.60±0.41

IC_{50} values denote the drug concentration that inhibits 50% of cell growth. Values represent the mean ± S.D. from 3 separate experiments.

mg/kg and 17.08 mg/kg, respectively. In general, experimental data above suggested that PST-3 inhibited cancer cell proliferation with high safety.

PST-3 binds to the colchicine binding site on microtubule

The antitubulin potency was examined by the docking study. First, the initial structure of the colchicine receptor was retrieved from the Protein Data Bank and then arranged for our study with ADT 1.5.6 by removing water molecules and the colchicine structure and adding polar hydrogens. The results of docking studies suggested PST-3 bound steady in the colchicine-binding domain between the α/β-tubulin (**Figure 2A**). Further studies on the inhibitor-tubulin complex (**Figure 2B**) reveals many hydrogen bonding and hydrophobic interactions, which is essential for the binding mode. The 2-(3, 4-dimethoxy)-benzoylthiophene moiety of PST-3 located in a polar cavity composed of A Leu-248, Thr-179, Asn-258, Lys-254, Ala-180, Glu-183, Asn-101, and Gln-11. Furthermore, the oxygen atom at the 4-methoxy group of the benzene ring of PST-3 (H-bond acceptor) established hydrogen bonding with residue Asn-101. The docking score of PST-3 (-10.0 kcal/mol) was close to colchicine (-10.1 kcal/mol). Thus, PST-3, which has a new structure, binding the colchicine-binding site of tubulin, and could provide some novel leading compound with great potential.

PST-3 induces morphological changes, disrupts the structure of microtubule in cells and inhibits tubulin polymerization

Due to its pivotal role of microtubules in maintaining cell structure, we investigated the effects of PST-3 on tubulin polymerization in intact cells. Immunocytochemistry visualization of cells showed that a complete tubule network was formed in α-tubulin and β-tubulin, which extended to the lamellipodium in cells of the control group. PST-3 treatment for BT549 (**Figure 3A**) and MDA-MB-468 (**Figure 3B**) cells lead to obvious damage in both α-tubulin and β-tubulin, as well as cellular structure change and the cell membrane forms a circle. As PST-3 could damage the network of tubulins of cells, we investigated if PST-3 can inhibit tubulin polymerization in a cell-free system. Bovine brain tubulin (> 97% pure) was incubated with PST-3, absorbance was recorded at 340 nm to be the indicator of tubulin polymerization. Docetaxel stabilizes the tubulins molecule, and the nucleation period is greatly reduced; the develop speed was increased. Besides, the ultimate polymer is larger than the mass of the tubulin destruction agent colchicine, which could reduce the growth rate and cut down the ultimate polymer mass. As **Figure 3C** shows, PST-3 inhibited tubulin polymerization by 92%. In addition, PST-3 inhibited tubulin polymerization in a concentration-dependent manner (IC_{50} = 5.31 μM, **Figure 3D**). Under the same experimental conditions, the IC_{50} for PST-3 is close to the IC_{50} of colchicine (4.25 μM). No obvious changes of α-tubulin and β-tubulin were observed in BT549 and MDA-MB-468 cell lines after treating with PST-3 at the IC_{50} concentrations, respectively (**Figure 3E**). Thus, our studies suggested that PST-3 could induce morphological changes and networks disruption of tubulins in BT549 and MDA-MB-468 cells without changing the expression of α-tubulin and β-tubulin.

PST-3 arrests BT549 and MDA-MB-468 cells in G2/M phase

Since suppression of tubulin polymerization finally results in cell cycle arrest and cell apoptosis, we then determined whether PST-3 would change cell cycle distribution through flow cytometry. BT549 and MDA-MB-468 cells were exposed to 15 μM (IC_{50}) of PST-3 for multiple durations (0, 24, 48, and 72 hours). The effect of PST-3 on cell cycle was studied through flow cytometry. **Figure 4A** and **4B** are indicating that PST-3 induced G2/M arrest in the way of time-dependent in BT549 and MDA-MB-468 cells. PST-3 (15 μM, 0.1% DMSO) arrested BT549 and MDA-MB-468 cells in

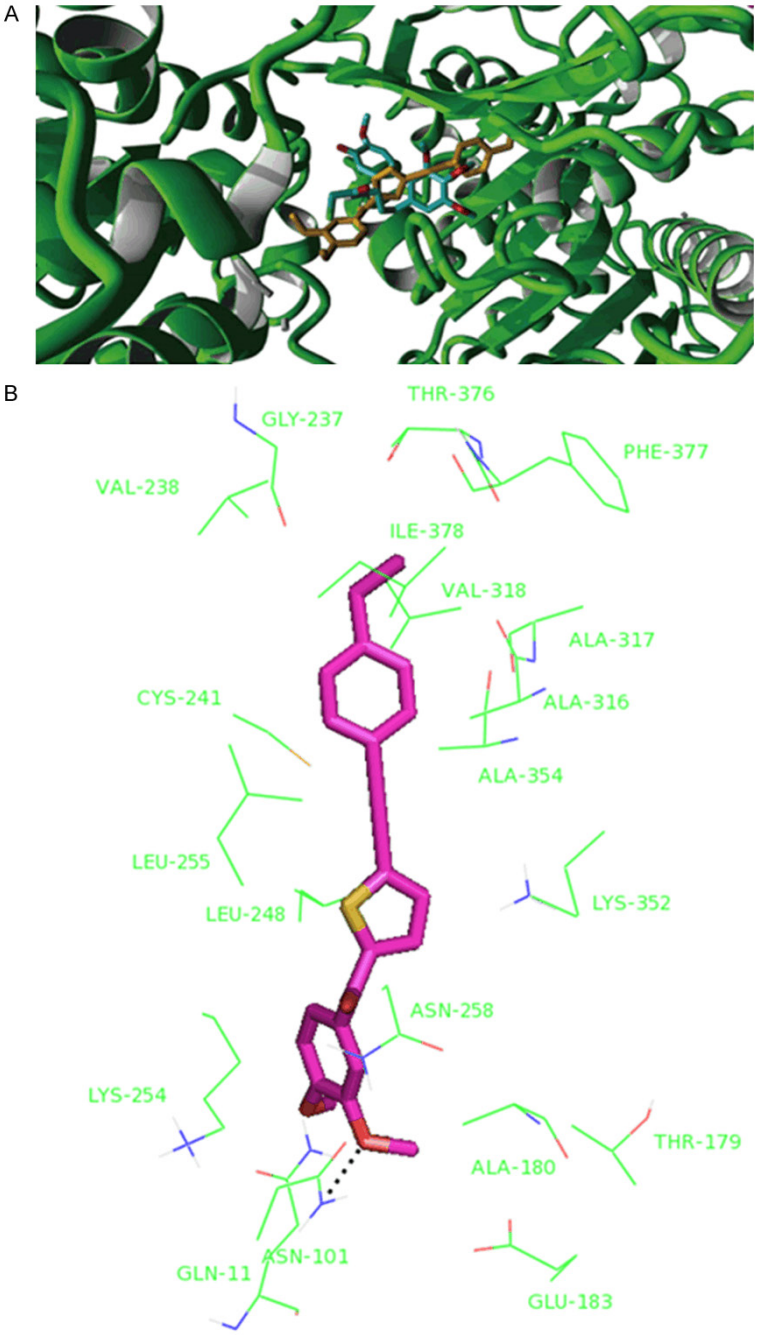

Figure 2. PST-3 and its interaction with the colchicine site receptor. PST-3 and Colchicine structure interacting with the colchicine site receptor. Colchicine site receptor is colored green; PST-3 is colored brown; Colchicine is colored cyan (A). PST-3 interaction with residues on the colchicine site receptor (B).

G2/M phase after 24 h treatment and MDA-MB-468 cells in G2/M phase after 48 h treatment. At the same time, a characteristic hypodiploid DNA peak (sub-G1) occurred in 36 hours post-treatment, meaning the presence of apoptotic cells. Further, Western blot was performed to determine the effects of PST-3 on the expression of cell cycle regulatory proteins. Data in **Figure 4C** demonstrated that treatment of BT549 and MDA-MB-468 cells with PST-3 resulted in the increase of Cyclin B in protein level, while Cyclin D1, Cyclin E and Cyclin H made no change. The expression of p21 was up-regulated at 24 hours in BT549 cells and 48 hours in MDA-MB-468 cells. These results further prove the blockage effect of PST-3 on G2/M phase.

PST-3 treatment leads to alteration in the expression levels of apoptotic proteins

To study the effect of PST-3 on the apoptosis of BT549 and MDA-MB-468 cells, BT-549 and MDA-MB-468 cells were treated with 15 μM (IC_{50} concentration) PST-3 for different times (0, 24, 48 and 72 hours). The results showed that PST-3 induced BT549 (**Figure 5B**, **5C**) and MDA-MB-468 (**Figure 5A**, **5D**) cells apoptosis in a time-dependent manner. Further, Western blot was performed to determine the effects of PST-3 on the expression of Apoptosis-related protein. The results are shown in **Figure 5E**, PST-3 treatment leads to reduced phosphorylation of p-Akt (T308) in BT549 and MDA-MB-468 cells. There was no significant change in the expression of total protein AKT. In addition, p-ERK 1/2, a key protein in the mitogen-activated protein kinase (MAPK) pathway, was also down-regulated after PST-3 treatment. Poly ADP-ribose polymerase (PARP) is an indicator of the intrinsic pathway of apoptosis. After

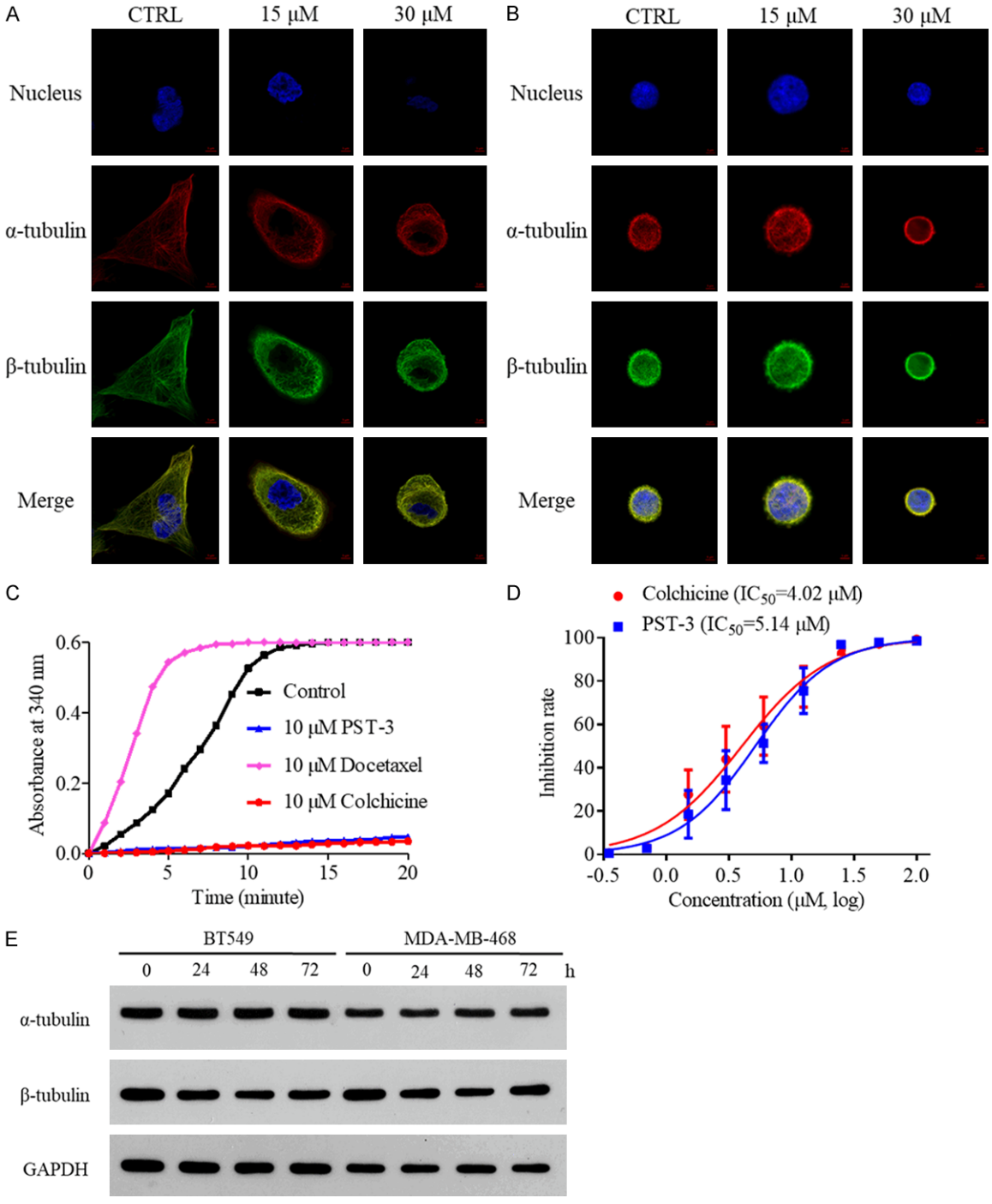

Figure 3. PST-3 induces morphological changes, disrupts the structure of microtubule in cells and inhibits tubulin polymerization. Effect of PST-3 on tubulin in BT549 cells (A) and MDA-MB-468 cells (B). Cells were seeded on glass coverslips, incubated with PST-3 (15 μM or 30 μM) for 6 h, fixed, and processed for confocal microscopy. PST-3 compound inhibits microtubule assembly *in vitro* (C). Purified tubulin in a reaction buffer was incubated at 37°C in the absence (control) or presence of 10 μM colchicine, docetaxel, or PST-3 compound. Tubulin polymerization inhibitory activity of PST-3 compound and colchicine (D). IC_{50} values denote the compound concentration that inhibits 50% of cell growth. Effect of PST-3 expression levels of α-tubulin and β-tubulin in BT549 and MDA-MB-468 cells (E). Cells were treated with PST-3 (15 μM) for different time points (0, 24, 48 and 72 h).

PST-3 treatment, PARP is cleaved and activated. Compared with the control group, the expression of Bax increased while the expression of Bcl-2 decreased.

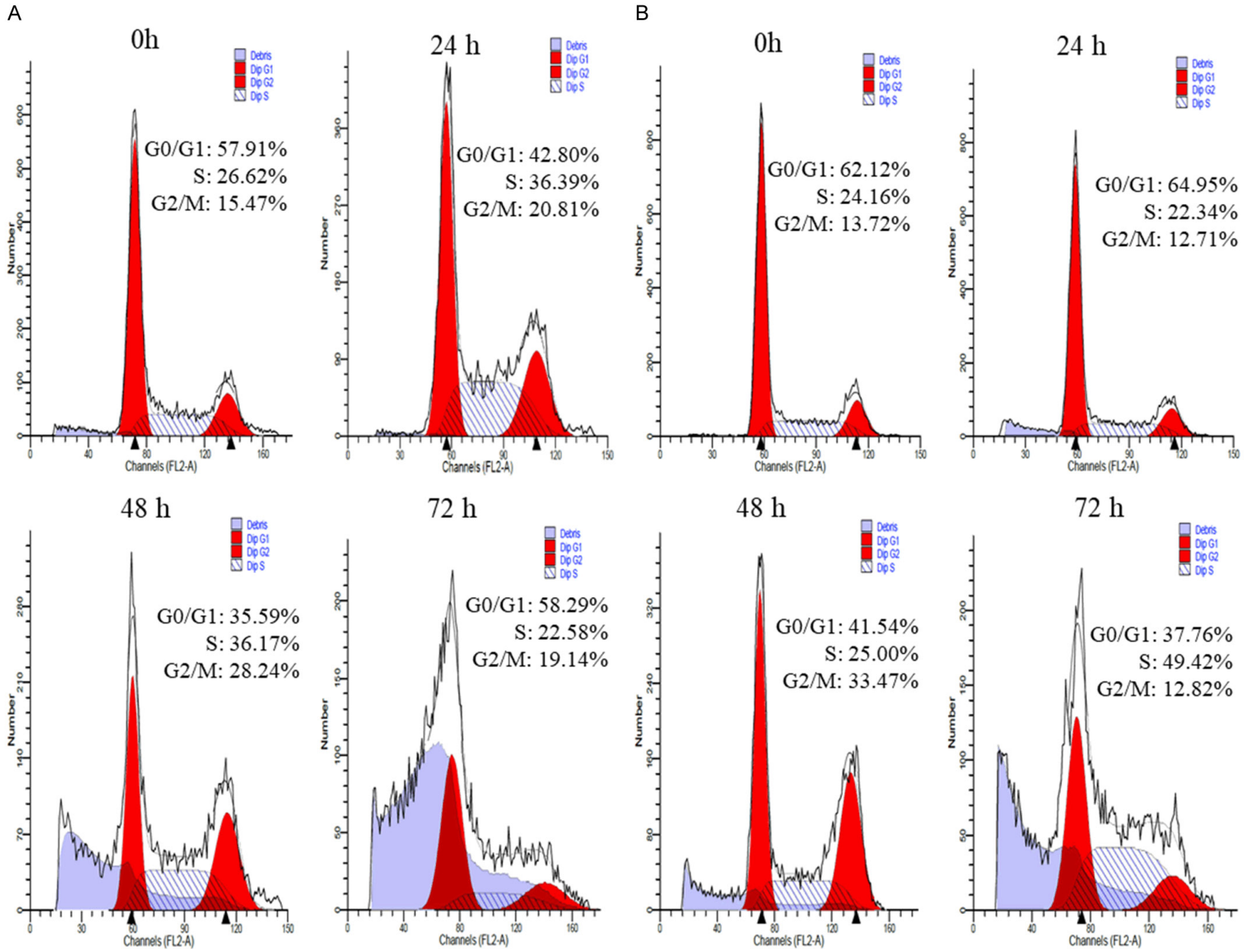
A
0h
G0/G1: 57.91%
S: 26.62%
G2/M: 15.47%
24 h
G0/G1: 42.80%
S: 36.39%
G2/M: 20.81%
48 h
G0/G1: 35.59%
S: 36.17%
G2/M: 28.24%
72 h
G0/G1: 58.29%
S: 22.58%
G2/M: 19.14%
B
0h
G0/G1: 62.12%
S: 24.16%
G2/M: 13.72%
24 h
G0/G1: 64.95%
S: 22.34%
G2/M: 12.71%
48 h
G0/G1: 41.54%
S: 25.00%
G2/M: 33.47%
72 h
G0/G1: 37.76%
S: 49.42%
G2/M: 12.82%
Debris
Dip G1
Dip G2
Dip S
Number
Channels (FL2-A)

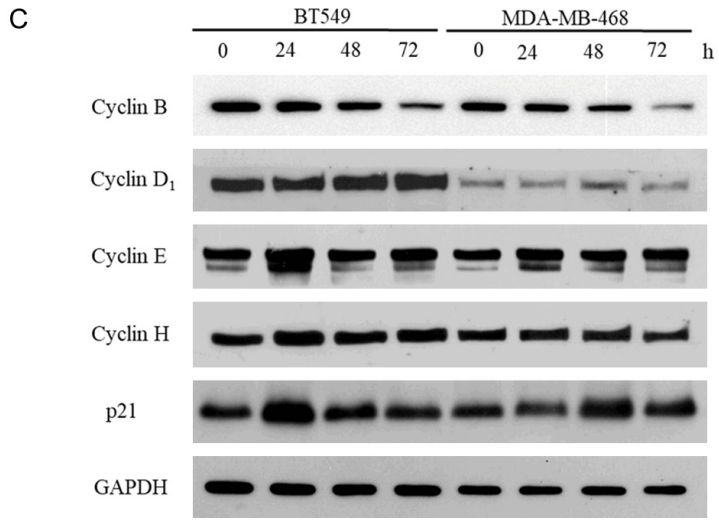

Figure 4. Effect of PST-3 treatment on cell cycle progression of BT549 (A) and MDA-MB-468 cells (B). Cells were treated with PST-3 (15 μM) for different time points (0, 24, 48 and 72 h). Cell cycle distribution was analyzed by flow cytometry after staining the cells with PI. The concentration of PST-3 selected was based on the IC_{50} value. Western blot analyzed Cyclin B, Cyclin D1, Cyclin E, Cyclin H and p21 proteins expression level in BT549 and MDA-MB-468 cells treated with 15 μM PST-3 for different time points (C).

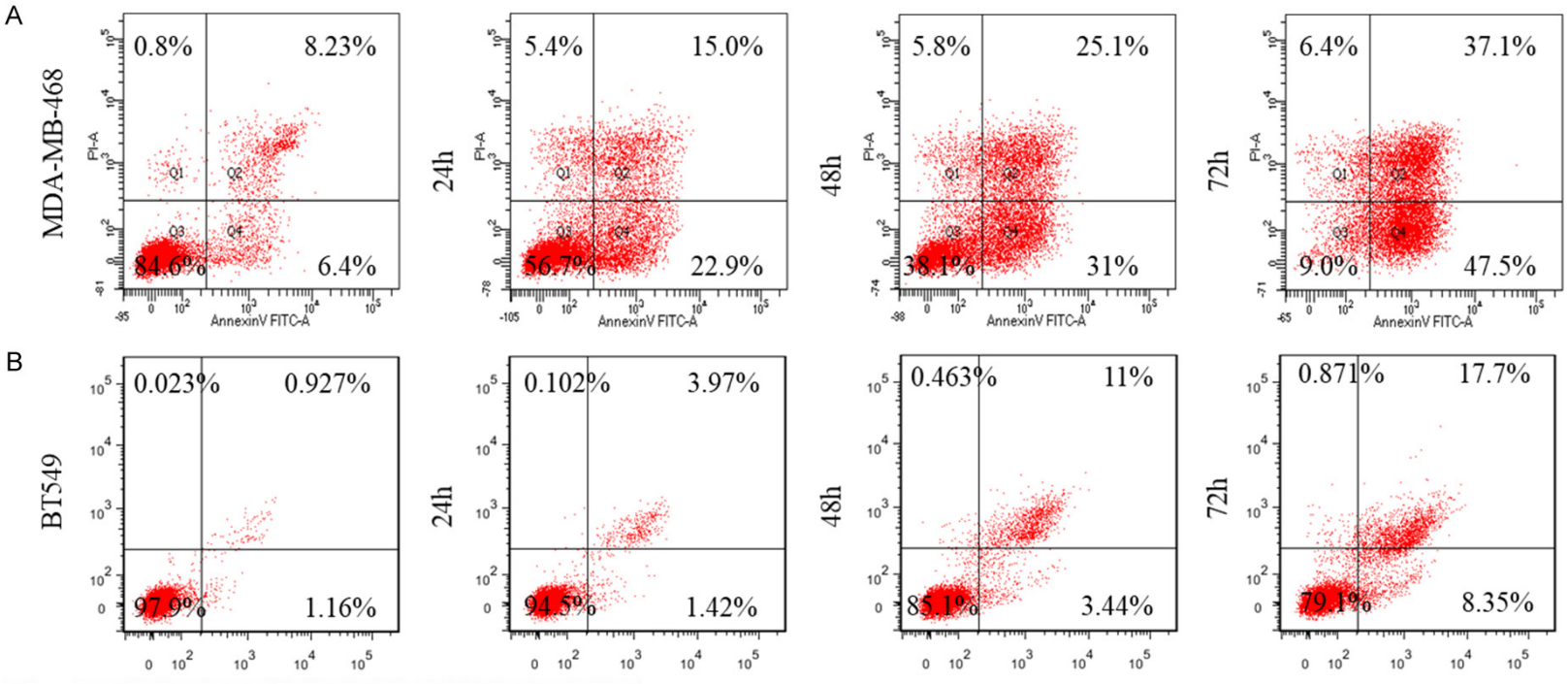

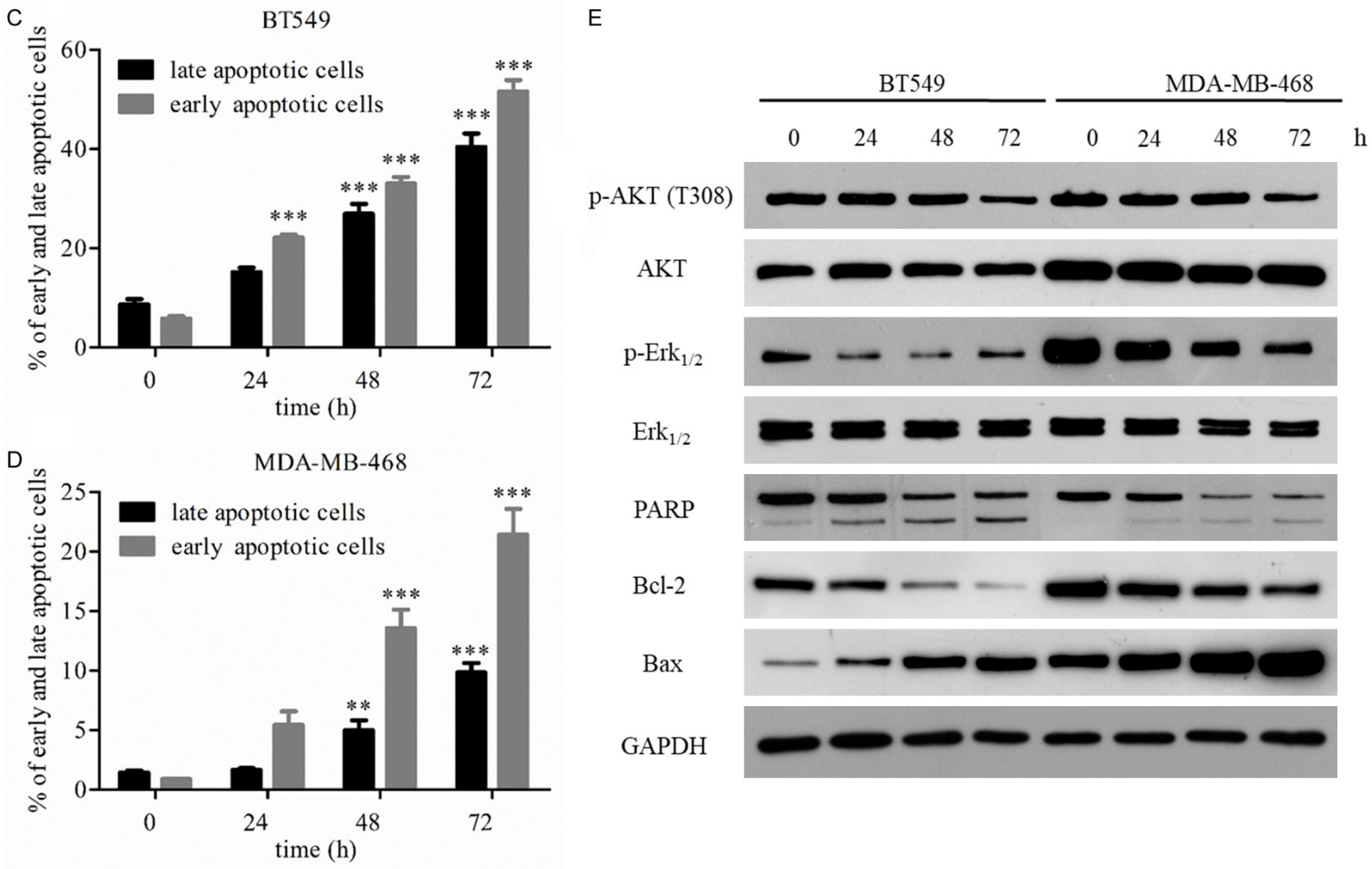

Figure 5. The effect of PST-3 on apoptotic. Effect of PST-3 treatment on the induction of apoptosis in MDA-MB-468 (A) and BT549 (B) cell. BT549 and MDA-MB-468 cells were treated with PST-3 (15 μM) for different time points (24, 48 and 72 h). Annexin V-FITC and PI staining was used to evaluate the effect of PST-3 on BT549 and MDA-MB-468 cells. In each panel, the lower left quadrant shows cells that were negative for both PI and Annexin V-FITC staining. The upper left quadrant shows PI-positive cells, representing necrotic cells. The lower right quadrant shows Annexin V-positive cells, which represent cells in the early apoptotic stage. The upper right quadrant shows both Annexin V- and PI-positive cells, which represent cells in the late stage of apoptosis and necrosis. Quantitative data of the effect of PST-3 on the induction of BT549 (C) and MDA-MB-468 (D) cell apoptosis. Expression levels of apoptotic proteins in BT549 and MDA-MB-468 cell lines upon treatment with PST-3 (E). The symbol ** represents $P < 0.01$ as compared to vehicle; the symbol *** represents $P < 0.001$ as compared to control group.

In vivo PK profile of PST-3

Single-dose of PST-3 (60 mg/kg) was administered intraperitoneally to mice to determine the pharmacokinetics (Supplementary Figure 2). The clearance value for PST-3 was over 90 ml/min/kg (the hepatic blood flow rate in mice) [38], indicated that apart from hepatic removal, PST-3 may have other degradation ways to eliminate. The half-life value for PST-3 was 5.6 hours, prompting that a high-frequency dosing regimen should be adopted to ensure its anticancer activity *in vivo*. The volume of distribution for PST-3 was moderate (5.3 L/kg) [38], while the exposure (AUC) value for PST-3 was 2.2 hr*μg/mL, suggesting that the low bioavailability for PST-3 (Supplementary Table 4). These PK data provided a reliable *in vivo* metabolic stability studies in animals.

PST-3 shows preferential growth inhibition in triple-negative breast cancer xenografts growth without neurotoxicity in vivo

We then studied the antitumor potential of PST-3 in two tumor models: MDA-MB-468 cell is TNBC cell line and MCF7 is non-TNBC cell lines. From the results of **Figure 6A** and **6B**, no significant body weight loss was observed in all experiment groups, which suggested low toxicity of PST-3 compound. As shown in **Figure 6C** and **6D**, tumor volumes in MDA-MB-468 xenografts increased to 1655.67± 399.07 mm^3 in the vehicle group, and 194.54±174.49 mm^3 in the PST-3 treated group by day 21. As shown in **Figure 6E** and **6F**, tumor volumes in MCF7 xenografts increased to 2695.68±899.85 mm^3 in the vehicle group and 1196.31±464.78 mm^3 in the PST-3 treated group by day 21. The *in vivo* effect (%T/C) for PST-3 compound in two tumor models were summarized in Supplementary Table 3. PST-3 elicited MDA-MB-468 tumor %T/C of 11.75%, whereas elicited MCF7 tumor %T/C of 44.38%. Results are demonstrating that PST-3 had preferential growth inhibition in triple-negative breast cancer xenografts growth.

To examine the possible neurotoxic effects of PST-3 *in vivo*, rotarod tests were performed. According to the data of *in vivo* pharmacodynamic experiments, 60 mg/kg [intraperitoneal injection, Captex200/Tween80 (1/4)] of PST-3 was selected to determine its influence on motor coordination. Keep the experimental parameters unchanged, a dose of 0.05 mg/kg application with colchicine was set as a positive control. Results in **Figure 6G** indicated colchicine shortens the duration (in seconds) that mice standing at the rotating rod, and there is a significant difference compared with the control group on the 9^{th} day ($P < 0.01$). However, it exhibited no significant difference between the PST-3 intervention groups, indicating that PST-3 caused no neurotoxicity in mice at doses that with anti-tumor effects. There is a theory that drugs could cause neurological toxicity if they cross the blood-brain barrier. Drugs could be recognized and excluded from the CNS by cellular efflux mechanisms such as P-glycoprotein (P-gp), which is highly expressed in cerebral capillaries. As showed in **Figure 6H**, PST-3 could bind with P-gp with the docking score of -8.0 kcal/mol, which is steadier than colchicine (-6.6 kcal/mol). To investigate whether PST-3 is a substrate of P-gp, drug-stimulated activity of P-gp ATPase was examined. As presented in **Figure 6I**, Verapamil and PST-3 induced an increase in activity of P-gp ATPase, which indicated that PST-3 is a substrate of P-gp. This result suggested that PST-3 could not cross the blood-brain barrier and lead to neurological toxicity.

Discussion

Currently, many potential microtubule stabilizers or destabilizers are synthesized, discovered, and evaluated every year [39]. Some microtubule inhibitors, including taxanes and the vinca alkaloids, have already entered the clinical application and reached the commercial stage [22]. Many tubulin inhibitors cause significant neurotoxicity during treatment, leading to clinical termination [39]. The phenomenon mentioned above can be exemplified by the Cryptophycins, a class of reagents prepared by total synthesis or obtained from cyanobacteria [40]. Due to significant neurotoxicity, there lack apparent effect in patients with advanced NSCLC receiving cryptophycin 52 (also called LY355703), although some diseases stabilizations were observed [40, 41]. The development of novel antitubulin agents without neurological toxicity is the priority for the optimization of compounds targeting tubules. In this study, PST-3 induced cytotoxicity in all detected tumor cell lines in the way of concen-

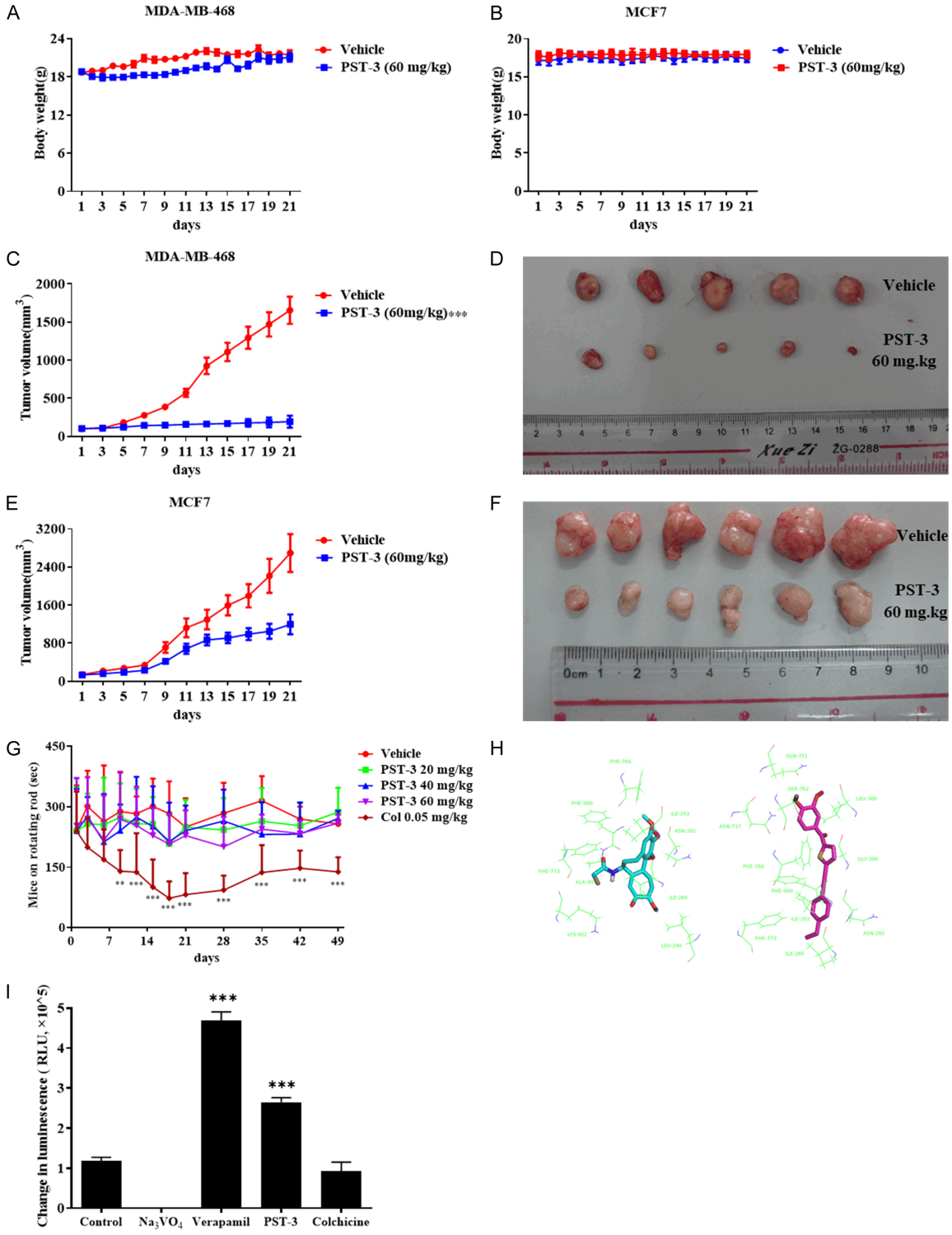

Figure 6. PST-3 compound shows preferential growth inhibition in triple-negative breast cancer xenografts growth without neurotoxicity. The mice transplanted with xenografts were randomly divided into two groups and administered injection of PST-3 (60 mg/kg, i.p.) or vehicle daily. Relative body weight (A, B) and tumor volume (C, E) is expressed as mean ± SD (n = 5 or 6 per group). Image of tumors treated with vehicle and PST-3 (60 mg/kg, i.p.) (D, F). Time of mice on rotating rod. PST-3 (20, 40 and 60 mg/kg), colchicine (0.5 mg/kg), and vehicle were given intraperitoneally daily (G, n = 8). PST-3 (left panel) and Colchicine (right panel) structure interacting with P-gp (H). Effect of PST-3 on P-gp ATPase activity. (I) The symbol ** represents $P < 0.01$ as compared to vehicle; the symbol *** represents $P < 0.001$ as compared to vehicle.

tration-dependent. At the same time, PST-3 showed low cytotoxicity on normal mammary epithelial cells MCF10A. Furthermore, PST-3 exhibited low toxicity in the acute toxicity study, which suggested that PST-3 may be developed as a novel compound with lesser toxicity on normal cells. Rotarod assay was conducted to investigate the peripheral neurotoxicity of PST-3 [42, 43]. Mice receiving PST-3 treatment did not show significant motor coordination impairment compared with the control group. In the positive control, the colchicine treatment group showed a shorter time to stand at the rotating rod, indicating neurotoxicity. To study the delayed neurotoxicity of PST-3, we repeated the study by 30 days later when the treatment was stopped. Our results demonstrated that the duration of the PST-3 treatment group mice to stand at the rotating rod recovered to the baseline. However, the ability of the colchicine treatment group can return either to the baseline neither vehicle treatment group, demonstrating that neurotoxicity is only partially reversible after treatment has stopped. The above results provide convincing evidence that we have developed a new compound without neurological toxicity. Since the microtubules of neurons are primarily responsible for the transport of vital molecules along the axons, which being bind with might suppress the transport of molecules, thus leading to peripheral neurotoxicity [44]. Therefore, if the difference between the microtubule skeleton of peripheral nerve and tumor cells are able identified, this will be helpful in explaining the neurotoxicity reduction of PST-3. These theories require further investigation [22]. Sagopilone (ZK-EPO), a kind of epothilones, is a microtubule-stabilizing agent in exploitation for the therapy of solid tumors. It's reported that the central nervous system (CNS) toxicity of Sagopilone partly because it was not P-gp efflux pump substrates, therefore is able to cross the blood-brain barrier [45, 46].

Many drug candidates have encountered problems associated with high metabolic clearance, chemical instability, and peripheral neurotoxicity during development [47-49]. PK studies were carried with PST-3 in mice, and results demonstrated that PST-3 has the characteristics of high clearance rate, short half-life, a moderate volume of distribution and low AUC. Considering the results of high clearance and short half-period in mice, high-frequency dosing regimen was adopted.

Docking studies indicated that PST-3 bound to colchicine binding pocket in microtubule by situating in a polar cavity formed by Leu-248, Thr-179, Asn-258, Lys-254, Ala-180, Glu-183, Asn-101, and Gln-11 and forming a hydrogen bond interaction with Asn-101. Besides, immunofluorescence microtubule detection and tubulin polymerization assay suggested that PST-3 disrupted the microtubule networks in cancer cells and suppressed the polymerization of microtubule *in vitro*. Experimental results above demonstrate that PST-3 inhibit tubulin polymerization and interacts with the colchicine binding site of tubulin. Otherwise, we synthesized PST-3 using a simple 3-step procedure in our laboratory because of its small molecular weight (376 Dalton) and the relatively simple structure, offering a novel way for fast and high production synthesis.

PST-3 treatment led to a phase arrest of G2/M in both BT549 and MDA-MB-468 cells in the time dependent way, subsequently enhanced the accumulation of cells in Sub G1 phase, suggesting the activation of cell death-related pathways. Studies in the past few years proved that many different chemotherapeutic drugs lead to cell cycle blocked. For example, through targeting microtubule formation, paclitaxel and nocodazole result in G2/M cell cycle arrest, and apoptosis subsequently [50, 51]. Furthermore, express changes of checkpoint proteins related to cell cycle dynamics may also clarify the role of PST-3 on cell cycle arrest. Cyclin B1 participate in G2/M cell cycle progression is a G2/M conversion regulatory molecule [52]. PST-3 treatment caused the reduction of cyclin B1 protein expression, further explaining the effect of PST-3 on cell cycle arrest.

Triple negative breast cancer (TNBC) is an invasive tumor subtype with poor prognosis, distant metastasis rate as well as high recurrence rate. TNBC is a clinical subtype of breast cancer which is negative for progesterone receptor (PR), estrogen receptor (ER), and human epidermal growth factor receptor-2 (HER-2) [53, 54]. The prognosis of patients with TNBC depends primarily on the reaction to chemotherapy. Patients with poor response to chemotherapy have a higher risk of recurrence

after surgery [55]. However, there is still a lack of effective targeted treatment for TNBC, which means systemic chemotherapy become the only choice for TNBC patients [56]. In our study, the IC_{50} values for PST-3 compound were lower in Hs578T, BT549, MDA-MB-231 and MDA-MB-468 cells (TNBC cells) than MCF7 and T47D cells (non-TNBC cells) which indicated that PST-3 were more sensitive to TNBC cells. PST-3 compound also showed preferential growth inhibition in triple-negative breast cancer xenografts growth *in vivo*. The results suggest that PST-3 can be developed as specific chemotherapy agents for those triple-negative breast cancer patients.

In summary, we have demonstrated that PST-3 compound is a novel antitubulin compound binds to the colchicine-binding site of the microtubule. In addition, PST-3 is an effective anticancer agent both *in vitro* and *in vivo*. The efficacy studies demonstrated that PST-3 compound has preferential growth inhibition in triple-negative breast cancer xenografts growth. Importantly, PST-3 compound exhibited no neurotoxicity *in vivo*. The anticancer effects of PST-3 compound, as well as the low neurotoxicity obtained in our research provide a foundation for preclinical studies, suggesting that this novel compound might have therapeutic potential for clinical treatment of cancer. However, further experiments are needed to clarify the preferential mechanism of PST-3 in triple-negative breast cancer. Moreover, future structural modifications are required to improve the activity of PST-3 while maintaining its low neurotoxicity characteristics.

Acknowledgements

This research was supported by the National Natural Science Foundation, China (project No. 81473246), Guangdong Science and Technology Department (project NO. 2017A0303-13734) and Guangdong Science and Technology Department (project No. 2017A05050-1020). We declare there are no financial and personal relationships with other people or organizations that can inappropriately influence our work. We would like to thank all the participants of this study for their exceptional cooperation as well as valuable contributions.

Disclosure of conflict of interest

None.

Address correspondence to: Lin Lv and Zhipeng Chen, School of Pharmaceutical Science, Southern Medical University, Guangzhou 510515, People's Republic of China. E-mail: lynnlv@smu.edu.cn (LL); czpwyq2008@163.com (ZPC)

References

[1] Germann UA. P-glycoprotein-a mediator of multidrug resistance in tumour cells. Eur J Cancer 1996; 32A: 927-944.
[2] Howard J and Hyman AA. Dynamics and mechanics of the microtubule plus end. Nature 2003; 422: 753-758.
[3] Jordan MA, Thrower D and Wilson L. Mechanism of inhibition of cell proliferation by Vinca alkaloids. Cancer Res 1991; 51: 2212-2222.
[4] Kruczynski A and Hill BT. Vinflunine, the latest Vinca alkaloid in clinical development. A review of its preclinical anticancer properties. Crit Rev Oncol Hematol 2001; 40: 159-173.
[5] Lehnert M. Clinical multidrug resistance in cancer: a multifactorial problem. Eur J Cancer 1996; 32A: 912-920.
[6] Mattern J. Drug resistance in cancer: a multifactorial problem. Anticancer Res 2003; 23: 1769-1772.
[7] Parker AL, Kavallaris M and McCarroll JA. Microtubules and their role in cellular stress in cancer. Front Oncol 2014; 4: 153.
[8] Rose WC. Taxol: a review of its preclinical in vivo antitumor activity. Anticancer Drugs 1992; 3: 311-321.
[9] Yvon AM, Wadsworth P and Jordan MA. Taxol suppresses dynamics of individual microtubules in living human tumor cells. Mol Biol Cell 1999; 10: 947-959.
[10] Adak A, Mohapatra S, Mondal P, Jana B and Ghosh S. Design of a novel microtubule targeted peptide vesicle for delivering different anticancer drugs. Chem Commun (Camb) 2016; 52: 7549-7552.
[11] De O and Chatterji BP. Marine derived anticancer drugs targeting microtubule. Recent Pat Anticancer Drug Discov 2017; 12: 102-127.
[12] Hadfield JA, Ducki S, Hirst N and McGown AT. Tubulin and microtubules as targets for anticancer drugs. Prog Cell Cycle Res 2003; 5: 309-325.
[13] Honore S, Pasquier E and Braguer D. Understanding microtubule dynamics for improved cancer therapy. Cell Mol Life Sci 2005; 62: 3039-3056.
[14] Jordan A, Hadfield JA, Lawrence NJ and McGown AT. Tubulin as a target for anticancer drugs: agents which interact with the mitotic spindle. Med Res Rev 1998; 18: 259-296.
[15] Jordan MA and Kamath K. How do microtubule-targeted drugs work? An overview. Curr Cancer Drug Targets 2007; 7: 730-742.

[16] Singh P, Rathinasamy K, Mohan R and Panda D. Microtubule assembly dynamics: an attractive target for anticancer drugs. IUBMB Life 2008; 60: 368-375.
[17] Sparreboom A, van Tellingen O, Nooijen WJ and Beijnen JH. Preclinical pharmacokinetics of paclitaxel and docetaxel. Anticancer Drugs 1998; 9: 1-17.
[18] Brouhard GJ and Rice LM. The contribution of alphabeta-tubulin curvature to microtubule dynamics. J Cell Biol 2014; 207: 323-334.
[19] Hu MJ, Zhang B, Yang HK, Liu Y, Chen YR, Ma TZ, Lu L, You WW and Zhao PL. Design, synthesis and molecular docking studies of novel indole-pyrimidine hybrids as tubulin polymerization inhibitors. Chem Biol Drug Des 2015; 86: 1491-1500.
[20] Pellegrini F and Budman DR. Review: tubulin function, action of antitubulin drugs, and new drug development. Cancer Invest 2005; 23: 264-273.
[21] Bates D and Eastman A. Microtubule destabilising agents: far more than just antimitotic anticancer drugs. Br J Clin Pharmacol 2017; 83: 255-268.
[22] Dumontet C and Jordan MA. Microtubule-binding agents: a dynamic field of cancer therapeutics. Nat Rev Drug Discov 2010; 9: 790-803.
[23] Heinz DW, Schubert WD and Hofle G. Much anticipated--the bioactive conformation of epothilone and its binding to tubulin. Angew Chem Int Ed Engl 2005; 44: 1298-1301.
[24] Jin X, Yang YD, Chen K, Lv ZY, Zheng L, Liu YP, Chen SH, Yu CH, Jiang XY, Zhang CY and Li YM. HDMCP uncouples yeast mitochondrial respiration and alleviates steatosis in L02 and hepG2 cells by decreasing ATP and H2O2 levels: a novel mechanism for NAFLD. J Hepatol 2009; 50: 1019-1028.
[25] Lee FY, Borzilleri R, Fairchild CR, Kamath A, Smykla R, Kramer R and Vite G. Preclinical discovery of ixabepilone, a highly active antineoplastic agent. Cancer Chemother Pharmacol 2008; 63: 157-166.
[26] Perez EA. Microtubule inhibitors: differentiating tubulin-inhibiting agents based on mechanisms of action, clinical activity, and resistance. Mol Cancer Ther 2009; 8: 2086-2095.
[27] Simoni D, Romagnoli R, Baruchello R, Rondanin R, Grisolia G, Eleopra M, Rizzi M, Tolomeo M, Giannini G, Alloatti D, Castorina M, Marcellini M and Pisano C. Novel A-ring and B-ring modified combretastatin A-4 (CA-4) analogues endowed with interesting cytotoxic activity. J Med Chem 2008; 51: 6211-6215.
[28] Akhmanova A and Steinmetz MO. Control of microtubule organization and dynamics: two ends in the limelight. Nat Rev Mol Cell Biol 2015; 16: 711-726.
[29] Li W, Sun H, Xu S, Zhu Z and Xu J. Tubulin inhibitors targeting the colchicine binding site: a perspective of privileged structures. Future Med Chem 2017; 9: 1765-1794.
[30] Lu Y, Chen J, Xiao M, Li W and Miller DD. An overview of tubulin inhibitors that interact with the colchicine binding site. Pharm Res 2012; 29: 2943-2971.
[31] Canta A, Chiorazzi A and Cavaletti G. Tubulin: a target for antineoplastic drugs into the cancer cells but also in the peripheral nervous system. Curr Med Chem 2009; 16: 1315-1324.
[32] Argyriou AA, Koltzenburg M, Polychronopoulos P, Papapetropoulos S and Kalofonos HP. Peripheral nerve damage associated with administration of taxanes in patients with cancer. Crit Rev Oncol Hematol 2008; 66: 218-228.
[33] Peng L, Bu Z, Ye X, Zhou Y and Zhao Q. Incidence and risk of peripheral neuropathy with nab-paclitaxel in patients with cancer: a meta-analysis. Eur J Cancer Care (Engl) 2017; 26.
[34] Zhang W, Shi S, Jiang J, Li X, Lu H and Ren F. LncRNA MEG3 inhibits cell epithelial-mesenchymal transition by sponging miR-421 targeting E-cadherin in breast cancer. Biomed Pharmacother 2017; 91: 312-319.
[35] Ravelli RB, Gigant B, Curmi PA, Jourdain I, Lachkar S, Sobel A and Knossow M. Insight into tubulin regulation from a complex with colchicine and a stathmin-like domain. Nature 2004; 428: 198-202.
[36] Tentler JJ, Tan AC, Weekes CD, Jimeno A, Leong S, Pitts TM, Arcaroli JJ, Messersmith WA and Eckhardt SG. Patient-derived tumour xenografts as models for oncology drug development. Nat Rev Clin Oncol 2012; 9: 338-350.
[37] Zheng YB, Gong JH, Liu XJ, Wu SY, Li Y, Xu XD, Shang BY, Zhou JM, Zhu ZL, Si SY and Zhen YS. A novel nitrobenzoate microtubule inhibitor that overcomes multidrug resistance exhibits antitumor activity. Sci Rep 2016; 6: 31472.
[38] Davies B and Morris T. Physiological parameters in laboratory animals and humans. Pharm Res 1993; 10: 1093-1095.
[39] Jordan MA and Wilson L. Microtubules as a target for anticancer drugs. Nat Rev Cancer 2004; 4: 253-265.
[40] D'Agostino G, del Campo J, Mellado B, Izquierdo MA, Minarik T, Cirri L, Marini L, Perez-Gracia JL and Scambia G. A multicenter phase II study of the cryptophycin analog LY355703 in patients with platinum-resistant ovarian cancer. Int J Gynecol Cancer 2006; 16: 71-76.
[41] Edelman MJ, Gandara DR, Hausner P, Israel V, Thornton D, DeSanto J and Doyle LA. Phase 2 study of cryptophycin 52 (LY355703) in patients previously treated with platinum based chemotherapy for advanced non-small cell lung cancer. Lung Cancer 2003; 39: 197-199.

[42] Bacher G, Nickel B, Emig P, Vanhoefer U, Seeber S, Shandra A, Klenner T and Beckers T. D-24851, a novel synthetic microtubule inhibitor, exerts curative antitumoral activity in vivo, shows efficacy toward multidrug-resistant tumor cells, and lacks neurotoxicity. Cancer Res 2001; 61: 392-399.
[43] Nakai R, Iida S, Takahashi T, Tsujita T, Okamoto S, Takada C, Akasaka K, Ichikawa S, Ishida H, Kusaka H, Akinaga S, Murakata C, Honda S, Nitta M, Saya H and Yamashita Y. K858, a novel inhibitor of mitotic kinesin Eg5 and antitumor agent, induces cell death in cancer cells. Cancer Res 2009; 69: 3901-3909.
[44] Dumontet C and Sikic BI. Mechanisms of action of and resistance to antitubulin agents: microtubule dynamics, drug transport, and cell death. J Clin Oncol 1999; 17: 1061-1070.
[45] Arnold D, Voigt W, Kiewe P, Behrmann C, Lindemann S, Reif S, Wiesinger H, Giurescu M, Thiel E and Schmoll HJ. Weekly administration of sagopilone (ZK-EPO), a fully synthetic epothilone, in patients with refractory solid tumours: results of a phase I trial. Br J Cancer 2009; 101: 1241-1247.
[46] Schmid P, Kiewe P, Possinger K, Korfel A, Lindemann S, Giurescu M, Reif S, Wiesinger H, Thiel E and Kuhnhardt D. Phase I study of the novel, fully synthetic epothilone sagopilone (ZK-EPO) in patients with solid tumors. Ann Oncol 2010; 21: 633-639.
[47] Fukuda DS, Mabe JA and Brannon DR. Production of substituted L-tryptophans by fermentation. Appl Microbiol 1971; 21: 841-843.
[48] Lin JH and Lu AY. Role of pharmacokinetics and metabolism in drug discovery and development. Pharmacol Rev 1997; 49: 403-449.
[49] Windebank AJ. Chemotherapeutic neuropathy. Curr Opin Neurol 1999; 12: 565-571.
[50] Jordan MA, Wendell K, Gardiner S, Derry WB, Copp H and Wilson L. Mitotic block induced in HeLa cells by low concentrations of paclitaxel (taxol) results in abnormal mitotic exit and apoptotic cell death. Cancer Res 1996; 56: 816-825.
[51] Milas L, Hunter NR, Kurdoglu B, Mason KA, Meyn RE, Stephens LC and Peters LJ. Kinetics of mitotic arrest and apoptosis in murine mammary and ovarian tumors treated with taxol. Cancer Chemother Pharmacol 1995; 35: 297-303.
[52] Li Y, Liu D, Lopez-Paz C, Olson BJ and Umen JG. A new class of cyclin dependent kinase in Chlamydomonas is required for coupling cell size to cell division. Elife 2016; 5: e10767.
[53] Dietze EC, Sistrunk C, Miranda-Carboni G, O'Regan R and Seewaldt VL. Triple-negative breast cancer in African-American women: disparities versus biology. Nat Rev Cancer 2015; 15: 248-254.
[54] Newman LA. Breast cancer disparities: socioeconomic factors versus biology. Ann Surg Oncol 2017; 24: 2869-2875.
[55] Groheux D, Giacchetti S, Delord M, de Roquancourt A, Merlet P, Hamy AS, Espie M and Hindie E. Prognostic impact of 18F-FDG PET/CT staging and of pathological response to neoadjuvant chemotherapy in triple-negative breast cancer. Eur J Nucl Med Mol Imaging 2015; 42: 377-385.
[56] Schettini F, Giuliano M, De Placido S and Arpino G. Nab-paclitaxel for the treatment of triple-negative breast cancer: rationale, clinical data and future perspectives. Cancer Treat Rev 2016; 50: 129-141.

Supplementary Materials

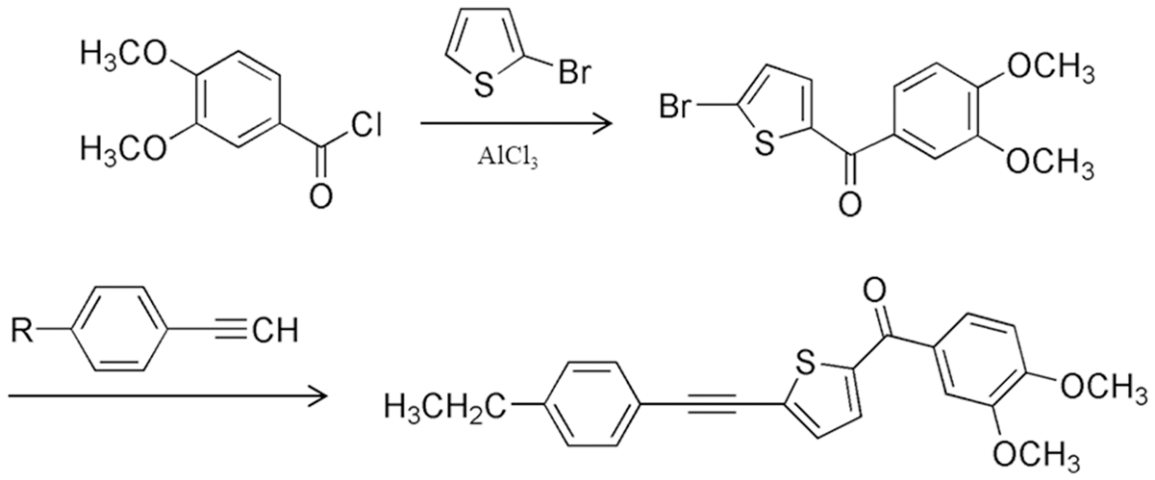

Supplementary Figure 1. Synthesis of PST-3.

Supplementary Table 1. Loss of body weight after 4 consecutive days of PST-3 i.p. dosing

Dose	5 mg/kg	10 mg/kg	20 mg/kg	40 mg/kg	60 mg/kg	80 mg/kg	100 mg/kg
Initial weight (g)	21.62	21.20	21.41	20.45	21.10	21.38	20.73
Final weight (g)	21.45	21.11	21.12	19.64	20.08	18.06	16.81
Loss of body weight	0.75%	0.41%	1.32%	3.96%	4.84%	15.56%	18.94%

Supplementary Table 2. Acute toxicity of PST-3 and colchicine administered intraperitoneally to mice

Dose of PST-3 (mg/kg)	Mortality (D/T)		Mortality (%)	Dose of colchicine (mg/kg)	Mortality (D/T)		Mortality (%)
	Female	Male			Female	Male	
0	0/5	0/5	0	0	0/5	0/5	0
2.15	0/5	0/5	0	2.15	0/5	0/5	0
21.5	0/5	0/5	0	21.5	4/5	2/5	60
215	0/5	0/5	0	215	5/5	5/5	100
2150	0/5	0/5	0	2150	5/5	5/5	100
LD_{50}	> 2150 mg/kg			LD_{50}	17.08 mg/kg		

D/T: dead/treated mice.

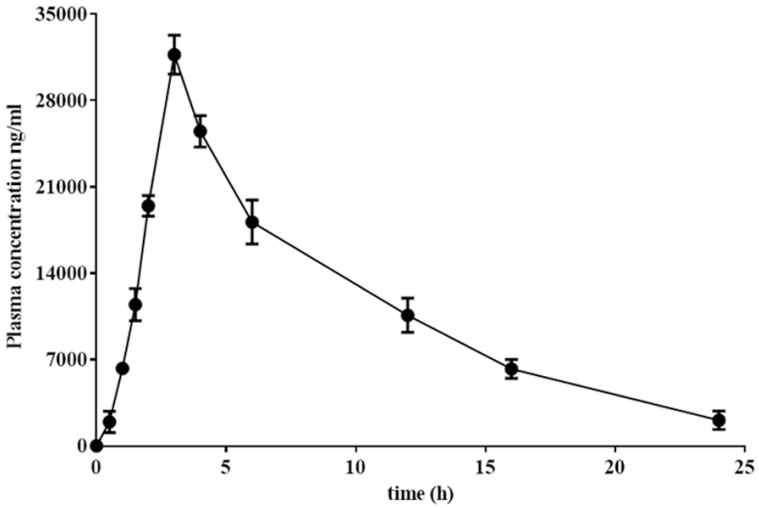

Supplementary Figure 2. Pharmacokinetic studies of PST-3 in mice. Concentration-time curve of PST-3 in ICR mice (n = 5); bars, SD. 60 mg/kg PSR-3 was administrated intraperitoneally with the formulation 0.1% Captex200/ Tween80 (1/4).

Supplementary Table 3. Pharmacokinetic parameters of PST-3

Parameter	Unit	PST-3
CL	mL/min/kg	143
$t_{1/2}$	hr	5.6
Vss	L/kg	5.3
AUC	hr*μg/mL	2.2

Supplementary Table 4. *In vivo* treatment of human tumor xenografts

Compound	Dosage (mg/kg)	Xenograft model	%T/C
Vehicle	NA	MDA-MB-468	100
PST-3	60	MDA-MB-468	11.75
Vehicle	NA	MCF7	100
PST-3	60	MCF7	44.38